

A deep near-infrared view of the Galactic globular cluster 2 MASS GC 02^{★,★★}

J. Borissova¹, V. D. Ivanov², A. W. Stephens³, M. Catelan⁴, D. Minniti⁴, and G. Prieto⁵

¹ Departamento de Física y Astronomía, Facultad de Ciencias, Universidad de Valparaíso, Ave. Gran Bretaña 1111, Playa Ancha, Casilla 5030, Valparaíso, Chile

e-mail: jura.borissova@uv.cl

² European Southern Observatory, Av. Alonso de Córdoba 3107, Casilla 19, Santiago 19001, Chile

e-mail: vivanov@eso.org

³ Gemini Observatory, 670 N. Aóhoku Place, Hilo, HI 96720, USA

e-mail: astephens@gemini.edu

⁴ Departamento de Astronomía y Astrofísica, Pontificia Universidad Católica de Chile, Av. Vicuña Mackenna 4860, 782-0436 Macul, Santiago, Chile

e-mail: [mcatelan;dante]@astro.puc.cl

⁵ Carnegie Institution of Washington, Las Campanas Observatory, Av. Colina El Pino s/n, Casilla 601, La Serena, Chile

e-mail: gprieto@lco.cl

Received 4 April 2007 / Accepted 8 August 2007

ABSTRACT

Context. We have obtained deep infrared images and K -band spectra of the Galactic globular cluster 2 MASS GC 02. A variable star search has also been carried out.

Aims. Some basic physical properties of the cluster, such as metallicity, reddening, distance modulus and radial velocity, are derived.

Methods. These measurements are based on an analysis of the $J - K_s$ versus K_s color–magnitude diagram of the cluster. Spectroscopically derived metallicities and radial velocities of 15 stars are presented. In addition, periods and amplitudes are provided for five RR Lyrae stars discovered in the field.

Results. The cluster is moderately metal-rich and has a relatively high radial velocity. Its horizontal branch appears to be predominantly red, though our photometry cannot rule out the presence of a blue component as seen in NGC 6388 and NGC 6441. Similar to these two clusters, the detected RR Lyrae stars in GC 02 have anomalously long periods for the cluster’s moderately high metallicity, which suggests that it too is an Oosterhoff type III cluster.

Conclusions. Comparison with the existing kinematic and abundance information for the Galactic globular clusters shows that GC 02 most probably belongs to the bulge sub population, although an inner halo association cannot be ruled out.

Key words. Galaxy: globular clusters: general – Galaxy: globular clusters: individual: 2 MASS GC 01 – Galaxy: abundances – Galaxy: globular clusters: individual: 2 MASS GC 02 – Galaxy: globular clusters: individual: NGC 6388 – Galaxy: globular clusters: individual: NGC 6441

1. Introduction

The knowledge and accurate measurement of such fundamental parameters as age, metallicity, distance from the Sun, reddening, etc. for the Galactic globular cluster system plays a key role in studies of the global properties of the Galaxy and its subcomponents. Correlations among their intrinsic parameters, on the other hand, can help us better understand the Galaxy’s formation and evolution. There are currently 150 known globular clusters in the Milky Way, according to the 2003 version of the Harris (1996)

catalog. In the latest review by Bica et al. (2006), three more recently discovered/re-classified clusters have been added, and the whole sample of Galactic globular clusters at the moment contains data for 153 objects (see their Table 1). Over the last few years, several “new” globular clusters have been discovered. In particular, Hurt et al. (2000), using data from the Two Micron All Sky Survey (2MASS), discovered two new globular clusters, 2 MASS GC 01 and 2 MASS GC 02 (hereafter GC 01 and GC 02, respectively), which are now included in the Bica et al. (2006) catalog. They are both located very close (in projection) to the Galactic center (within 10 deg) and are virtually invisible at optical wavelengths: Hurt et al. derived a visual extinction of $A_V = 21.5 \pm 1.0$ mag for GC 01 and $A_V = 18.0 \pm 1.0$ mag for GC 02, thus making infrared observations the only viable alternative to study them. The Galactic globular cluster census is still incomplete, as recently shown by Froebrich et al. (2007), who reported on a “new” globular cluster, FSR 1735, in the inner parts of our galaxy; and also by Koposov et al. (2007), who identified two extremely low-luminosity globular clusters in the

* The spectroscopy is based on observations collected with the Very Large Telescope of the European Southern Observatory within Observing Program 73.D-0158(A). The photometry is based on data gathered with the 6.5-m Magellan telescopes and the Henrietta Swope 1.0 m telescope, located at Las Campanas Observatory, Chile.

** A table with the individual J and K_s photometry is only available in electronic form at the CDS via anonymous ftp to cdsarc.u-strasbg.fr (130.79.128.5) or via <http://cdsweb.u-strasbg.fr/cgi-bin/qcat?J/A+A/474/121>

Milky Way halo in the Sloan Digital Sky Survey Data Release 5 images.

A preliminary analysis of follow-up near-infrared photometry for GC 01 and GC 02 clusters was reported by Ivanov et al. (2000, 2002) and Borissova et al. (2002). From $J-K_s$ vs. K_s color–magnitude diagrams, these authors estimated some of the cluster parameters. In particular, based on the slope of the red giant branch, and using the Ivanov et al. (2002) calibrations, they calculated photometric metallicities of $[Fe/H] = -1.19 \pm 0.38$ and -0.66 ± 0.17 for GC 01 and GC 02, respectively. King model fits of the surface brightness profiles of these clusters suggest a core radius $\log(r_c) = 1.63$ and concentration parameter $c = r_t/r_c = 1.41$ for GC 01, while GC 02 is more concentrated, with $\log(r_c) = 1.4$, $\log(r_h) = 1.54$, $\log(r_t) = 1.31$ arcmin and $c = 1.60$ (Borissova et al. 2002; note that r_t is the tidal radius, and that all radial distances, except the r_t are given in arcsec).

In this paper we present new deep IR photometry and the first spectroscopic measurements for GC 02. A variable star search is also reported. The paper is organized as follows: in Sect. 3 we report on the spectroscopically derived metallicities and radial velocities for 15 stars; in Sect. 4 we analyze the $J-K_s$ versus K_s color–magnitude diagram of the cluster; and in Sect. 5 the periods and amplitudes of 5 RR Lyrae stars are given. In the last section we compare the derived properties of GC 02 with the bulge, disk, and halo globular cluster systems in our galaxy.

2. Observation and data reduction

The K -band spectra were obtained with ISAAC UT1 (Moorwood et al. 1998) at the ESO-VLT. We used the SWS1-LW mode, with a 0.3 arcsec slit centered at $2.2 \mu\text{m}$ and spectral resolution 500. The exposure times were 10–15 min. We observed six slit positions, each of them containing at least two probable cluster members selected from the $J-K_s$ vs. K_s color–magnitude diagram of Ivanov et al. (2000). Since the slit length is 120 arcsec, in summary 31 stars fall into these six slit positions. They are shown in Fig. 1. Reductions were performed using standard IRAF¹ routines and the ISAAC pipeline. The spectra were extracted using the IRAF task `apall`. For each position along the slit a night sky spectrum was extracted using the same extraction parameters. The wavelength calibration from these 10–15 sky lines gives rms residuals typically in the 0.04–0.05 Å range. The spectra of the telluric stars were extracted and wavelength-calibrated in the same way. Each target spectrum was then divided by its corresponding standard star spectrum in order to correct for the atmospheric absorption features. The shape of the continuum was eliminated from the spectrum of each target by multiplying by an artificial blackbody continuum for a temperature of 14 000 K.

Infrared imaging observations were carried out on July 31, 2003 with the PANIC (Persson’s Auxiliary Nasmyth Infrared Camera, Martini et al. 2004) near-infrared imager on the 6.5-m Baade telescope at the Las Campanas Observatory. The instrument uses a 1024×1024 HgCdTe Hawaii detector array. The scale is $0.125 \text{ arcsec pixel}^{-1}$, giving a total field of view of 2.1×2.1 arcmin. The total integration time was 300 s both for the J and K_s bands. The stellar photometry of the flat-fielded, sky-subtracted and combined individual images was carried out using ALLSTAR in DAOPHOT II (Stetson 1994). The mean

¹ IRAF is distributed by the National Optical Astronomy Observatories, which is operated by the Association of Universities for Research in Astronomy, Inc. (AURA) under cooperative agreement with the National Science Foundation.

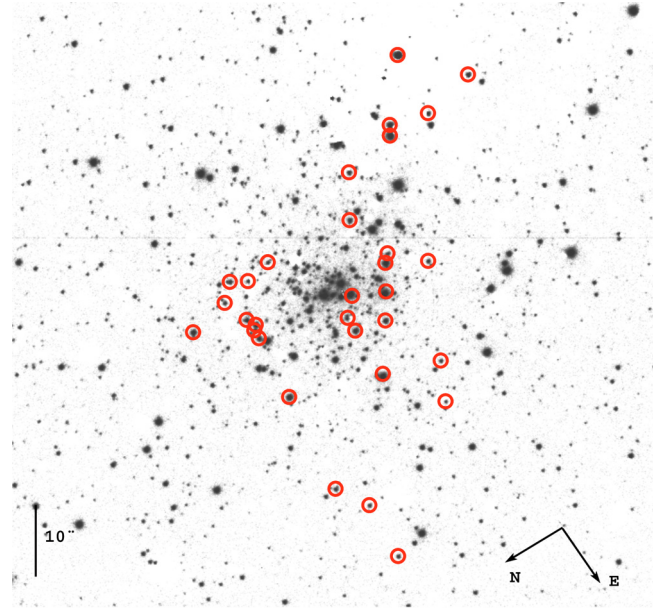


Fig. 1. All stars observed with ISAAC UT1 at the ESO-VLT. The field of view is 1.3×1.3 arcmin.

averaged internal photometric errors are 0.04 ± 0.02 for the J and K_s magnitudes brighter than 15 mag and 0.06 ± 0.03 for the fainter stars. We also added in quadrature an additional observational uncertainty of ~ 0.03 mag due to the sky background variations. The weather conditions were non-photometric, with typical seeing 1–1.2 arcsec, forcing us to calibrate the data by comparing our instrumental magnitudes with 2 MASS magnitudes, using of order 60–70 stars per image. The standard error values for the coefficients are 0.07 and 0.05 for the J and K_s zero points, and 0.02 and 0.03 for the color terms. In summary, our conservative estimate of the total external errors of our photometry is 0.05–0.06 mag. The completeness experiments show a 90% completeness limit at $K_s = 15.5$ mag. The final photometric list contains 2143 stars. The brightest stars (with $K_s < 10.5$ mag), which are saturated in our photometry, have been replaced with 2 MASS measurements.

During five consecutive nights (13–17) in July 2003, twelve epochs of K_s observations were obtained with C40IRC on the 1-m (40-inch) Swope telescope at Las Campanas Observatory. The C40IRC IR camera uses a Rockwell NICMOS-3 HgCdTe 256×256 array. The focal plane scale is 0.6 arcsec/pixel, with a total field size of 2.5×2.5 arcmin. The Swope frames were reduced in the same way as the PANIC images and transformed to the standard system independently using 20–30 stars in common with 2 MASS. The internal error of each measurement for the stars in GC 02 depends on the seeing and crowding conditions and is typically 0.04–0.05 mag for $K_s < 15$ mag.

3. K-band spectroscopy

From the whole sample of 31 stars with K -band spectra only 15 have $S/N \geq 30$. A sample of them is shown in Fig. 2.

The radial velocities of these fifteen stars were derived using the IRAF task `fxcor`, which uses a cross-correlation Fourier method. Since we did not observe any radial velocity standard, we used two stars from the literature as templates. The first one, BMB 181 (NGC 6522 NB 69), an M7 III star with $[Fe/H] = -0.21$ and $RV = 12 \pm 0.5 \text{ km s}^{-1}$, is taken from the stellar library of Ivanov et al. (2004), whereas the second template,

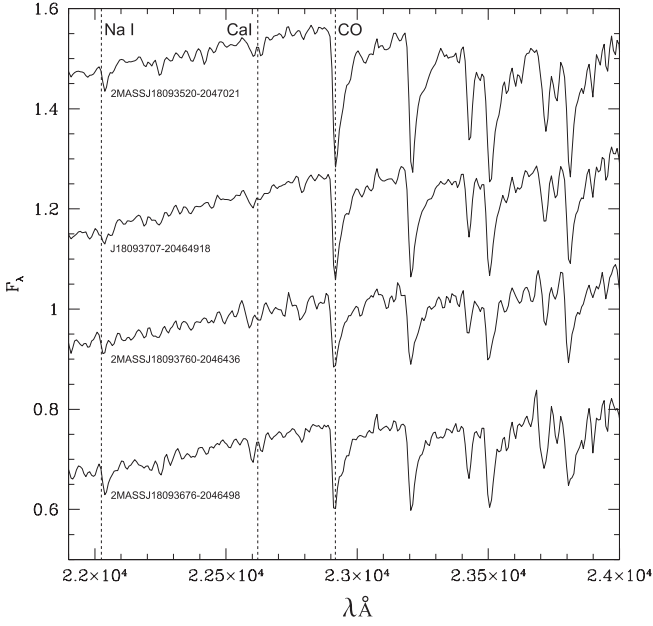


Fig. 2. A sample of reduced spectra for GC 02 stars. The different spectra have been arbitrarily shifted in monochromatic flux F_λ for clarity. The first, third and fourth spectra are labeled according to their 2MASS designation, while for the second star the RA and Dec (J2000) are given. The dashed lines indicate the wavelengths of the features measured in Table 1.

UK2III, is selected from the ISAAC “Library of Stellar Spectra for Spectrophotometric Calibration” (Pickles 1998). The radial velocities derived from each are given in Cols. 10 and 11 of Table 1. The mean value is given in Col. 12, while Col. 13 gives the dispersion around the mean. The membership of the stars is determined on the basis of the radial velocities histogram; twelve stars are accordingly found to be cluster members. They are marked in the last column of Table 1. The mean radial velocity value calculated from the cluster members is $RV = -238 \pm 36 \text{ km s}^{-1}$.

The metallicity was then calculated from the globular cluster metallicity indicator developed by Frogel et al. (2001). Their method is based on moderate-resolution near-IR spectroscopy in the K band of six to ten of the brightest giants in a cluster. They measured the equivalent widths of three features in the spectra, namely: $EW(\text{Na I } 2.21 \mu\text{m})$ and $EW(\text{Ca I } 2.26 \mu\text{m})$ atomic line blends and the EW of the first band head of CO ($2.29 \mu\text{m}$). The equivalent widths of these lines have been calibrated with spectra of more than 100 giant stars in 15 Galactic globular clusters with well-determined $[\text{Fe}/\text{H}]$ values. The technique is valid for globulars with $-1.8 < [\text{Fe}/\text{H}] < -0.1$ in the Harris (1996) metallicity scale, and reproduces the metallicities of the calibrating clusters to within ± 0.1 dex. The advantage of this method is that it can be used for heavily reddened globular clusters in crowded fields and it does not require a knowledge of any other cluster or stellar parameter, such as reddening, distance, or luminosity. We accordingly calculated our $[\text{Fe}/\text{H}]$ using Eq. (3) in Frogel et al. (2001), namely:

$$[\text{Fe}/\text{H}] = 0.182 \text{EW}(\text{Na}) + 0.0571 \text{EW}(\text{Ca}) + 0.0273 \text{EW}(\text{CO}) - 1.663.$$

The result is given in Col. 9 of Table 1. The mean value calculated for the cluster members is $[\text{Fe}/\text{H}] = -1.08 \pm 0.12$ in the Harris (1996) metallicity scale.

2MASS designation	RA(J2000) hh:mm:ss	Dec(J2000) deg:mm:ss	K_s	$J-K_s$	Na(2.20)	Ca(2.26)	CO(2.29)	[Fe/H]	RV(1) km s ⁻¹	RV(2) km s ⁻¹	RV km s ⁻¹	σ km s ⁻¹	Member
	18:09:34.60	-20:47:11.30	11.47	3.61	0.48	2.16	11.09	-1.15	-189	-170	-180	19	yes
	18:09:34.73	-20:47:03.28	12.02	5.27	4.37	4.40	8.53	-0.38	-331	-367	-349	32	no
	18:09:34.82	-20:46:48.64	12.09	3.6	1.95	2.10	8.1	-0.97	-281	-284	-283	6	yes
2MASSJ18093520-2047021	18:09:35.19	-20:47:02.28	9.42	4.08	1.20	3.67	5.99	-1.07	-245	-240	-243	8	yes
	18:09:35.19	-20:46:31.57	12.73	3.69	0.36	1.56	10.09	-1.23	-216	-218	-217	8	yes
	18:09:35.26	-20:46:27.62	12.71	3.61	1.80	1.53	8.96	-1.00	-178	-200	-189	22	yes
	18:09:35.27	-20:46:45.62	10.62	3.49	1.14	1.12	7.81	-1.18	-59	-74	-67	15	no
	18:09:35.32	-20:46:23.01	12.74	3.67	1.24	0.89	7.85	-1.17	-227	-276	-252	35	yes
	18:09:35.42	-20:46:16.76	11.06	3.84	1.27	1.27	10.92	-1.06	-227	-235	-231	11	yes
	18:09:35.85	-20:46:48.10	12.77	3.55	0.62	2.97	6.96	-1.19	-256	-275	-266	19	yes
	18:09:35.94	-20:46:47.15	10.77	3.01	3.66	3.64	20.99	-0.22	-123	-118	-121	8	no
2MASSJ18093649-2046441	18:09:36.60	-20:46:45.68	-	-	1.76	2.69	9.82	-0.92	-289	-290	-290	5	yes
2MASSJ18093676-2046498	18:09:36.78	-20:46:49.93	9.24	3.95	1.38	3.06	11.57	-0.92	-204	-198	-201	9	yes
	18:09:37.07	-20:46:49.18	11.32	3.78	0.99	1.56	4.09	-1.28	-271	-274	-273	7	yes
2MASSJ18093760-2046436	18:09:37.50	-20:46:43.62	9.89	3.97	2.19	1.49	7.48	-0.98	-229	-227	-228	6	yes

Table 1. Metallicity and radial velocities of the program stars.

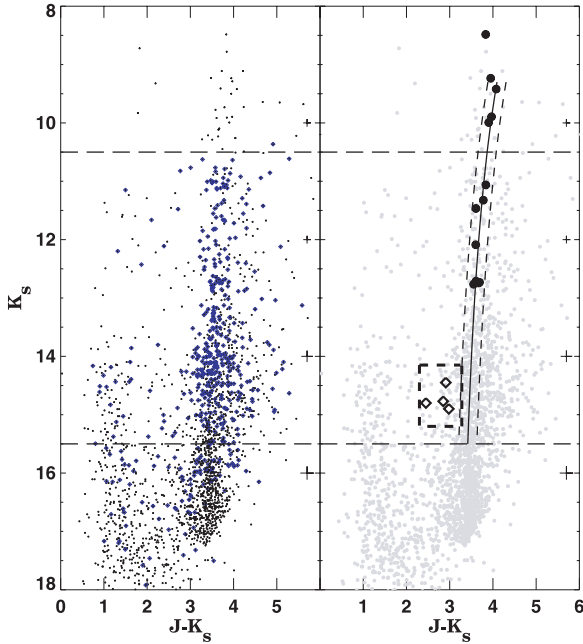


Fig. 3. K_s versus $J-K_s$ color–magnitude diagram for GC 02. The typical photometric errors for different magnitude bins are shown on the right as plus signs. In the left panel all measured stars are plotted as dots, and the stars within 30 arcsec from the cluster center are overplotted as diamonds. In the right panel the spectroscopically confirmed cluster members are marked with large dark circles. The RGB fiducial is shown by a solid line, with the 90% confidence level for the corresponding fit indicated as dashed lines (see text for details). The diamonds represent four probable RR Lyrae variable stars. The two horizontal dashed lines at $K_s = 10.5$ and $K_s = 15.5$ are the bright (replaced by 2MASS) and faint (50% completion) limits of the photometry.

4. Color–magnitude diagram

The $J-K_s$ versus K_s color–magnitude diagram is shown in Fig. 3. In the left panel all measured stars are plotted as small circles and the stars within 30 arcsec from the cluster center are overplotted as diamonds. In the right panel the spectroscopically confirmed cluster members are marked with large dark circles (see Sect. 3 for details), while the diamonds represent four probable RR Lyrae variable stars (see Sect. 5 for details). This new CMD is ~ 1.5 mag deeper than the one presented by Ivanov et al. (2000), thus allowing us a more detailed analysis of the physical parameters of the cluster.

As can be seen in Fig. 3, the cluster members are clearly separated from the bluer disk main sequence stars, although there is some contamination by field giants. The cluster members and field giants have $3 < J-K_s < 4$, while the disk main-sequence stars have $1 < J-K_s < 3$. The red giant branch (RGB) is well populated up to the tip. To separate (at least partially) the most probable RGB cluster members from the field stars we determined the mean ridgeline using the spectroscopically confirmed cluster members (see Sect. 3). The brightest spectroscopically confirmed cluster member is at the very center of GC 02, and is saturated even in our shortest exposure images. Its 2 MASS magnitude is uncertain because of crowding and the large pixel size in the 2MASS images. Therefore, this star is excluded from the calculation of the RGB fiducial. The best fit of the remaining 11 stars is shown in Fig. 3 as a solid line, and its 90% confidence interval is indicated with dashed lines. The fit was derived using a 3rd-order polynomial. We consider stars to be cluster members

if they lie within 30 arcsec of the cluster center, and fall within this 90% confidence interval.

The horizontal branch (HB) appears as a red clump, not well separated from the RGB, at $K_s \approx 14.3$ mag, and contains 10–15 stars within 30 arcsec of the cluster center. The HB region with probable RR Lyrae stars is plotted in Fig. 3 as a large dashed square. The subgiant region is poorly defined, and likewise it is impossible to determine the turn-off point of the cluster from our data.

The technique outlined in Ferraro et al. (2006) and Valenti et al. (2005, 2007) allows one to determine the reddening, distance modulus, and a global photometric metallicity of a globular cluster from its near-IR color–magnitude diagram, for two different chemical enrichment scenarios: i) disk-like ($[\alpha/\text{Fe}] = 0.3$ for $[\text{Fe}/\text{H}] \leq -1$ and $[\alpha/\text{Fe}]$ linearly decreasing to zero for $-1 \leq [\text{Fe}/\text{H}] \leq 0$); ii) bulge-like ($[\alpha/\text{Fe}] = 0.3$ over the whole metallicity range). As described in Ferraro et al. (2006), the procedure requires as input parameters the RGB slope and the RGB tip magnitude, as derived from the observed mean ridgeline in the K_s vs. $J-K_s$ diagram. In our case, for GC 02 the slope of the RGB was determined from the mean RGB line using the interval $11 < K_s < 14$. The tip of the RGB is determined in the following way: first, we check the brightest stars in our photometric list, which are saturated in our photometry and are taken from the 2MASS catalog. As mentioned before, the brightest spectroscopically confirmed cluster member has a 2MASS magnitude of $K_s = 8.48$, but this measurement includes two more unresolved companions, which are clearly visible on the VLT ISAAC acquisition images. For the same reason, it is not possible to check its variability on the Swope telescope images (see Sect. 5). The second brightest possible member has $K_s = 8.8$ and $J-K_s = 3.8$, and it lies on the limit of the 90% confidence interval in the color–magnitude diagram. The third brightest has $K_s = 9.1$ and $J-K_s = 4.2$; it lies within the confidence limits and did not show any night-to-night variations within the errors in our five consecutive nights of Swope observations. We accordingly adopted, for the K_s magnitude of the RGB tip, the mean value of $K_s = 9.0 \pm 0.2$, based on the weighted mean of the second and third brightest members.

The GC 02 parameters, calculated using Eqs. (3.1)–(3.4) and (4.1)–(4.4) in Ferraro et al. (2006), are given in Table 2.

Having thus obtained $(m-M)_K = 15.31$ and $E(J-K) = 3.01$, we performed a comparison with stellar isochrones provided by Pietrinferni et al. (2004). As can be seen from Fig. 4, on the basis of the existing photometry, without reaching the main-sequence turn-off point, it is not possible to discriminate between, say, 8 Gyr or 14 Gyr for $Z = 0.004$. Accordingly, all that we can state with confidence is that the cluster appears to be old, due to the presence of a well-developed RGB, as well as RR Lyrae stars (see the next section).

5. Variable stars

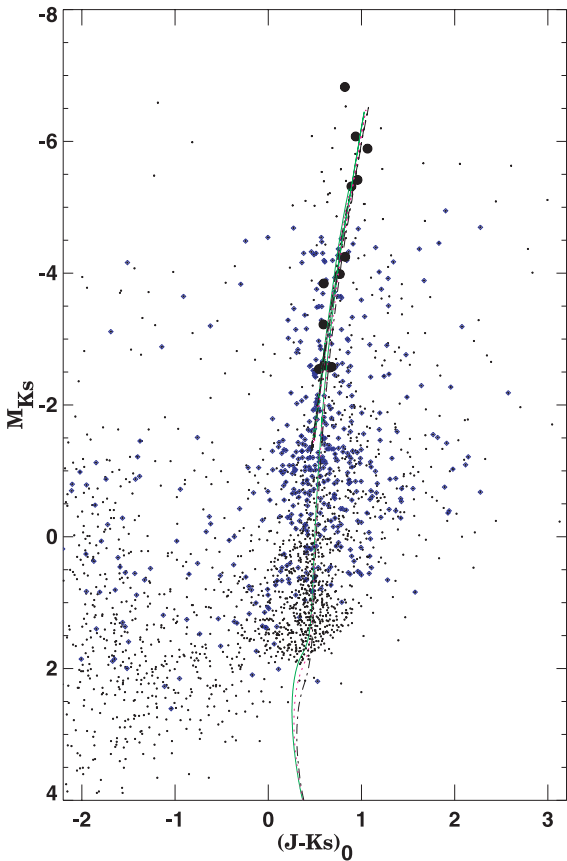
To search for candidate variable stars, we used night-to-night variations in the K_s magnitudes. The mean magnitude and error for every star from our photometric list based on 13 images (12 from the Swope telescope plus one from the Magellan-Baade telescope) were calculated. The mean error in magnitude for the stars brighter than $K_s = 15$ mag is 0.07 ± 0.05 . Then, we selected the candidates whose magnitudes changed by at least 2.5 times their errors. We choose this low threshold, because in general the amplitudes in K_s are much smaller than in the visual. To search for periods we used a period-finding program based on

Table 2. GC 02 parameters, as determined using the Ferraro et al. (2006) method.

Enrichment	RGB slope	[Fe/H]	[M/H]	$M_{K,\text{tip}}$	M_K	$E(B-V)$	A_V	A_K	$E(J-K)$	$(m-M)_0$
Disk	-0.082	-0.98	-0.82	-6.41	15.41	5.13	16.42	1.81	2.98	13.60
Bulge	-0.082	-0.98	-0.95	-6.31	15.31	5.19	16.61	1.83	3.01	13.48

Table 3. Pulsation parameters for the RR Lyrae stars.

Name	RA	Dec	$P(\text{days})$	Type	A_K	$\langle K_s \rangle$	$M_K(1)$	$M_K(2)$	$(m-M)_K$
V1	18:09:34.44	-20:47:48.8	0.8430	RRab	0.45	14.57	-0.98	-0.99	15.55
V2	18:09:36.43	-20:47:12.1	0.7105	RRab	0.42	14.77	-0.81	-0.82	15.58
V3	18:09:34.01	-20:46:57.0	0.8556	RRab	0.43	14.45	-0.99	-1.01	15.44
V4	18:09:39.86	-20:46:40.4	0.3555	RRc	0.28	14.80	-0.41	-0.42	15.21
V5	18:09:37.08	-20:46:57.0	0.3165	RRc	0.23	14.90	-0.30	-0.30	15.20

**Fig. 4.** M_{K_s} versus $(J-K_s)_0$ color-magnitude diagram of GC 02, with isochrones by Pietrinferni et al. (2004) for ages of 8 Gyr (solid line), 10 Gyr (dotted line) and 14 Gyr (dashed line) and metallicity $Z = 0.004$ superimposed. The symbols are as in Fig. 3.

Lafleur & Kinman’s (1965) “theta” statistic. Tentative periods for 5 candidate RR Lyrae variable stars were found in this way.

The pulsation parameters for RR Lyrae stars, together with their RA and Dec (J2000) coordinates, mean K_s magnitudes, and luminosity amplitudes, are listed in Table 3. The light curves are plotted in Fig. 5, and the finding chart is given in Fig. 6. The fit of the individual K_s -band phase points, shown in this figure as a solid line, was performed using the template light curves from Jones et al. (1996). The “light curve” of a non-variable star of similar magnitude is plotted for comparison.

We have found three RRab and two RRC Lyrae stars. Four of them are overplotted on the $J-K_s$ vs. K_s color-magnitude

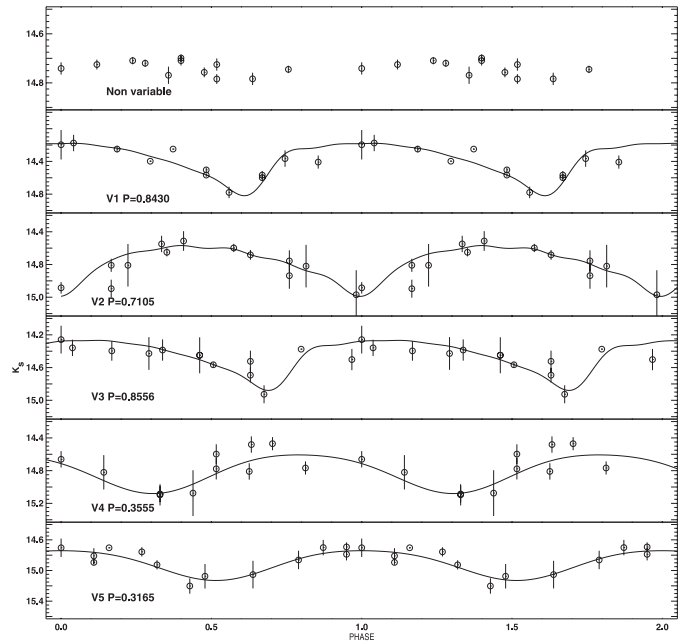
**Fig. 5.** K_s light curves for the probable RR Lyrae stars. The solid lines show the best-fitting template light curves from Jones et al. (1996). The “light curve” of a non-variable star of similar magnitude is plotted for comparison.

diagram shown in Fig. 3 (the probable variable V1 is omitted since it falls outside the PANIC FoV and we have no J magnitude for this star), and thus we can outline the probable intersection between the HB region and the instability strip. Note, however, that we have no mean J magnitudes for the RR Lyrae stars, so that we used the J magnitudes measured from the PANIC image taken at JD = 2452851.622. This leads to errors of up to 0.3–0.4 mag in the $J-K_s$ colors.

Obviously, our search for RR Lyrae stars is far from complete. Most of the stars in the HB region shown on the color-magnitude diagram are very close to the cluster center and thus unresolved in the Swope images. The probable RR Lyrae stars found here, on the other hand, are placed relatively far from the cluster center – we have only one star (V5) within 15 arcsec from the center, whereas the remainder are more than 30 arcsec away from the cluster center and thus outside the 35 arcsec half-light radius of the cluster (Borissova et al. 2002).

The positions of stars V1–V4 in the color-magnitude diagram appear consistent with membership in the cluster. The peak of the field RR Lyrae density distribution, however, is

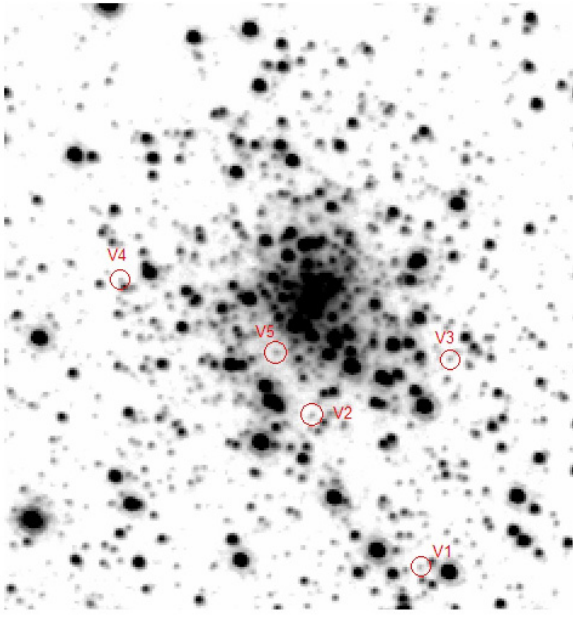


Fig. 6. K_s -band finding chart for the probable RR Lyrae stars. North is up, east is to the left. The field of view is 2.5×2.5 arcmin.

approximately at the cluster’s distance, so these stars could in principle also be field RR Lyrae variables. Since we have no spectra and thus lack radial velocities, we cannot settle this argument conclusively. However, it should be noted that the long periods that we have measured for the RRab stars (see below) are extremely unusual for field RR Lyrae of moderately high metallicity, but not so for moderately metal-rich globular cluster stars (e.g., Layden 1995; Sweigart & Catelan 1998; Catelan 2004, and references therein), thus strongly suggesting that, if these periods are correct, these stars are indeed cluster members.

Indeed, the average periods of the three candidate RRab stars is $\langle P_{ab} \rangle = 0.803$ d, which is remarkably long, and reminiscent of the cases of the “Oosterhoff type III” globular clusters NGC 6388 and NGC 6441 (e.g., Pritzl et al. 2000). While the number of RRab stars in GC 02 is admittedly small, small numbers of long-period RRab stars in moderately metal-rich globular clusters are becoming an increasingly common phenomenon, with other reported cases also being known in 47 Tucanae (NGC 104) and Terzan 5 (Catelan 2004, and references therein). As to the physical origin of these seemingly overluminous stars, the reader is referred to the recent discussion and references in Catelan (2007) and Catelan et al. (2006).

The last three columns of Table 3 list the absolute magnitudes of the RR Lyrae stars, as obtained using the period-luminosity (PL) relations derived by Cassisi et al. (2004 – $M_K(1)$ in the table) and Catelan et al. (2004, $M_K(2)$), as well as the distance modulus $(m - M)_K$, derived from the mean K -band magnitude. The average value for the three RRab stars gives $(m - M)_K = 15.40 \pm 0.18$ mag, in good agreement with values obtained from the RGB calibrations in the previous section. Since these PL relations depend on metallicity and HB type, we have adopted $[\text{Fe}/\text{H}] = -1$ and a predominantly red HB morphology. The periods of the RRC stars are fundamentalized by adding 0.128 to the logarithm of the period. Due to the possibility that the stars are overluminous, in analogy with what is seen in NGC 6388 and NGC 6441 (Catelan et al. 2006), the zero point of the PL relation would depend on the physical origin

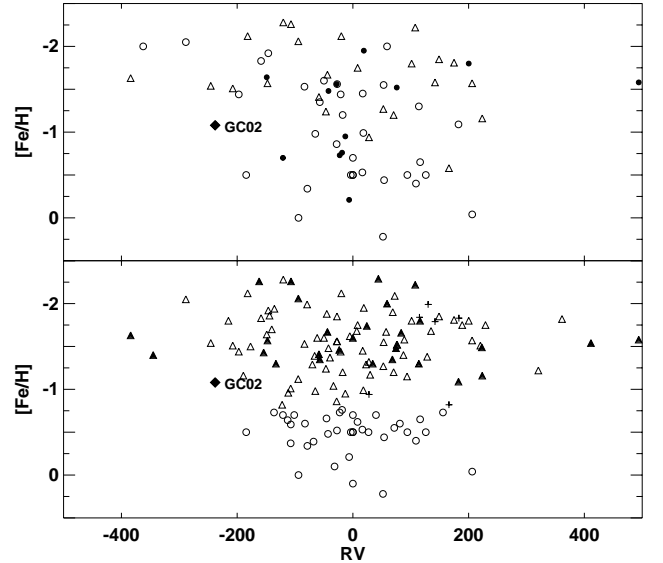


Fig. 7. Radial velocity vs. metallicity diagram for the globular clusters in the Galaxy, based on data from Harris (1996). GC 02’s position is shown as a filled diamond. *Upper panel:* classification of the globular clusters into the bulge (open circles), disk (filled circles), and halo sub-components (triangles), according to Pritzl et al. (2005). *Lower panel:* classification of the globular clusters from Mackey et al. (2005). The bulge/disk clusters are shown with open triangles, the old halo clusters with open circles, the young halo clusters with filled triangles, and the Sagittarius dSph clusters with crosses.

of the phenomenon, which is not yet clear (e.g., Catelan 2007, and references therein). For instance, according to the models of Catelan et al. (2004, see their Fig. 13), the zero point would change by ≈ 0.05 mag in K for an increase in the helium abundance by 0.05 (by mass fraction), thus adding an additional uncertainty in the distance modulus derived through this method of the order of 0.1 mag.

We checked also the brightest stars in the cluster for long-period, small-amplitude variability, but did not find night-to-night variations greater than 0.3 mag in K_s .

6. GC 02: a bulge, disk, or halo cluster?

In order to verify whether GC 02 is associated with the disk, bulge, or halo sub-populations of the Galaxy, we compared its position in the $[\text{Fe}/\text{H}]$ vs. radial velocity diagram with that occupied by other Galactic globular clusters, with data for the latter taken from the 2003 version of the Harris (1996) catalog (Fig. 7). We used two classification schemes. The first one is based on the work by Pritzl et al. (2005), who classified a sample of 45 Galactic globular clusters into bulge (Galactocentric distance $d < 2.7$ kpc), disk (thick and thin), and halo sub-components on the basis of the existing kinematic and abundance information (Fig. 7, upper panel). The second comes from Mackey & van den Bergh (2005), who classified the globular clusters in the Galaxy based on HB morphology and metallicity. They identified five main groups: bulge/disk clusters (37 objects), old halo clusters (70 objects), young halo clusters (30 objects), and Sagittarius dwarf spheroidal (dSph) clusters (7 objects). Both are shown in Fig. 7, lower panel). As can be seen, the scatter is very large. It seems that GC 02 may belong to the bulge sub-population of Galactic globular clusters, but the possibility that it is an inner halo cluster cannot be ruled out, due to its relatively high

radial velocity. Further information, especially orbit determination, is necessary to clarify this point.

7. Conclusions

GC 02 is an intermediate metal-rich globular cluster with a relatively high radial velocity. Its HB appears to be predominantly red, but the cluster does contain at least five RR Lyrae stars. Interestingly, the periods of the fundamental-mode (ab-type) RR Lyrae stars, which appear much longer than for typical field RR Lyrae stars of similar metallicity, are reminiscent of those seen in other globular clusters with moderately high metallicity. If this is confirmed with an enlarged sample of cluster RR Lyrae stars, the cluster will likely become the third bona-fide member of the “Oosterhoff III” group (Pritzl et al. 2000; Catelan 2007, and references therein).

Acknowledgements. J.B. and D.M. are supported by Fondap Center for Astrophysics 15010003. J.B. received partial support from Centro de Astrofísica de Valparaíso, Universidad de Valparaíso. Support for M.C. is provided by Proyecto Fondecyt Regular 1071002. We would like to thank Drs. E. Valenti, M. Zoccali, and L. Monaco for some useful comments.

References

- Alard, C. 2000, *A&A*, 144, 235
 Alard, C., & Lupton, R. H. 1998, *ApJ*, 503, 325
 Bica, E., Bonatto, C., Barbuy, B., & Ortolani, S. 2006, *A&A*, 450, 105
 Borissova, J., Ivanov, V. D., & Vanzi, L. 2002, in *Extragalactic Star Clusters*, ed. D. Geisler, E. K. Grebel, & D. Minniti (San Francisco: ASP), IAU Symp., 207, 107
 Catelan, M. 2004, in *Variable Stars in the Local Group*, ed. D. W. Kurtz, & K. R. Pollard (San Francisco: ASP), ASP Conf. Ser., 310, 113
 Catelan, M. 2007, in press [[arXiv:astro-ph/0507464](https://arxiv.org/abs/astro-ph/0507464)]
 Catelan, M., Pritzl, B. J., & Smith, H. A. 2004, *ApJS*, 154, 633
 Catelan, M., Stetson, P. B., Pritzl, B. J., et al. 2006, *ApJ*, 651, L133
 Castelli, F., Gratton, R. C., & Kurucz, R. L. 1997, *A&A*, 318, 841
 Cassisi, S., Castellani, M., Caputo, F., & Castellani, V. 2004, *ApJ*, 616, 498
 Ferraro, F., Valenti, E., & Origlia, L. 2006, *ApJ*, 649, 243
 Froebrich, D., Meusinger, H., & Scholz, A. 2007, *MNRAS*, 377, L54
 Frogel, J. A., Stephens, A., Ramírez, S., & DePoy, D. L. 2001, *AJ*, 122, 1896
 Girargi, L., Bertelli, L., Bressan, A., et al. 2002, *A&A*, 391, 195
 Harris, W. E. 1996, *AJ*, 112, 1487
 Hurt, R., Jarrett, T., Kirkpatrick, J., et al. 2000, *AJ*, 120, 1876
 Ivanov, V. D., Borissova, J., & Vanzi, L. 2000, *A&A*, 362, L1
 Ivanov, V. D., & Borissova, J. 2002, *A&A*, 390, 937
 Ivanov, V. D., Rieke, M., Engelbracht, C., et al. 2004, *ApJS*, 151, 387
 Jones, R., Carney, B., & Fulbright, J. 1996, *PASP*, 108, 877
 Koposov, S., de Jong, J., Belokurov, V., et al. 2007, *ApJ*, submitted [[arXiv:astro-ph/0706.0019](https://arxiv.org/abs/astro-ph/0706.0019)]
 Lafler, J., & Kinman, T. D. 1965, *ApJS*, 11, 216
 Layden, A. C. 1995, *AJ*, 110, 2312
 Martini, P., Persson, S. E., Murphy, D. C., et al. 2004, *Proc. SPIE*, 5492, 1653
 Mackey, A. D., & van den Bergh, S. 2005, *MNRAS*, 360, 631
 Moorwood, A., Cuby, J. G., Biereichel, P., et al. 1998, *The Messenger*, 94, 7
 Pickles, A. 1998, *AJ*, 110, 863
 Pritzl, B., Smith, H. A., Catelan, M., & Sweigart, A. V. 2000, *ApJ*, 530, L41
 Pritzl, B., Ven, K., & Irvin, M. 2005, *AJ*, 130, 2140
 Pietrinferni, A., Cassisi, S., Salaris, M., & Castellani, F. 2004, *ApJ*, 612, 168
 Stetson, P. B. 1994, *PASP*, 106, 250
 Sweigart, A. V., & Catelan, M. 1998, *ApJ*, 501, L63
 Valenti, E., Origlia, L., & Ferraro, F. R. 2005, *MNRAS*, 361, 272
 Valenti, E., Ferraro, F. R., & Origlia, L. 2007, *ApJ*, 133, 1287